

Synthesis and Spectroelectrochemical Studies of Mixed Heteroleptic Chelate Complexes of Ruthenium(II) with 1,8-Bis(2-pyridyl)-3,6-dithiaoctane (pdto) and Substituted 1,10-Phenanthrolines

Luis A. Ortiz-Frade,[†] Lena Ruiz-Ramírez,^{*,†} Ignacio González,[‡] Armando Marín-Becerra,[†] Manuel Alcarazo,^{†,§} José G. Alvarado-Rodríguez,^{||} and Rafael Moreno-Esparza[†]

Departamento de Química Inorgánica, Facultad de Química, Universidad Nacional Autónoma de México, Av. Universidad 3000, Ciudad Universitaria, México, D.F., 04510, Mexico, Departamento de Química, Universidad Autónoma Metropolitana-Iztapalapa, México, D.F., PO Box 55-534, 09340, Mexico, and Centro de Investigaciones Químicas, Universidad Autónoma del Estado de Hidalgo, U. Universitaria km. 4.5, Carretera Pachuca-Tulancingo 42074, Pachuca, Hidalgo, Mexico

Received July 4, 2002

Reaction of dichlorotris(triphenylphosphine) ruthenium(II) $[\text{RuCl}_2(\text{PPh}_3)_3]$ with 1,8-bis(2-pyridyl)-3,6-dithiaoctane (pdto), a (N_2S_2) tetradentate donor, yields a new compound $[\text{Ru}(\text{pdto})(\text{PPh}_3)\text{Cl}]\text{Cl}$ (**1**), which has been fully characterized. ^1H and ^{31}P NMR studies of **1** in acetonitrile at several temperatures show the substitution of both coordinated chloride and triphenylphosphine with two molecules of acetonitrile, as confirmed by the isolation of the complex $[\text{Ru}(\text{pdto})(\text{CH}_3\text{CN})_2]\text{Cl}_2$ (**2**). Cyclic voltammetric and spectroelectrochemical techniques allowed us to determine the electrochemical behavior of compound **1**. The substitution of the chloride and triphenylphosphine by acetonitrile molecules in the Ru(II) coordination sphere of compound **1** was also established by electrochemical studies. The easy substitution of this complex led us to use it as starting material to synthesize the substituted phenanthroline coordination compounds with (pdto) and ruthenium(II), $[\text{Ru}(\text{pdto})(4,7\text{-diphenyl-1,10-phenanthroline})]\text{Cl}_2 \cdot 4\text{H}_2\text{O}$ (**3**), $[\text{Ru}(\text{pdto})(1,10\text{-phenanthroline})]\text{Cl}_2 \cdot 5\text{H}_2\text{O}$ (**4**), $[\text{Ru}(\text{pdto})(5,6\text{-dimethyl-1,10-phenanthroline})]\text{Cl}_2 \cdot 5\text{H}_2\text{O}$ (**5**), $[\text{Ru}(\text{pdto})(4,7\text{-dimethyl-1,10-phenanthroline})]\text{Cl}_2 \cdot 3\text{H}_2\text{O}$ (**6**), and $[\text{Ru}(\text{pdto})(3,4,7,8\text{-tetramethyl-1,10-phenanthroline})]\text{Cl}_2 \cdot 4\text{H}_2\text{O}$ (**7**). These compounds were fully characterized, and the crystal structure of **4** was obtained. Cyclic voltammetric and spectroelectrochemical techniques allowed us to determine their electrochemical behavior. The electrochemical oxidation processes in these compounds are related to the oxidation of ionic chlorides, and to the reversible transformation from Ru(II) to Ru(III). On the other hand, a single reduction process is associated to the reduction of the substituted phenanthroline in the coordination compound. The $E_{1/2}$ (phen/phen⁻) and $E_{1/2}$ (Ru^{II}/Ru^{III}) for the compounds (**3–7**) were evaluated, and, as expected, the modification of the substituted 1,10-phenanthrolines in the complexes also modifies the redox potentials. Correlations of both electrochemical potentials with $\text{p}K_a$ of the free 1,10-phenanthrolines, λ_{max} MLCT transition band, and chemical shifts of phenanthrolines in these complexes were found, possibly as a consequence of the change in the electron density of the Ru(II) and the coordinated phenanthroline.

Introduction

Ru(II) polypyridine complexes have played a key role in the development of photochemistry and electron and energy

transfer. These complexes show fluorescence in the visible region, which has been used to study macromolecular assemblies useful in biochemistry and clinical diagnosis.^{1–8}

* To whom correspondence should be addressed. E-mail: lena@servidor.unam.mx.

[†] Universidad Nacional Autónoma de México.

[‡] Universidad Autónoma Metropolitana-Iztapalapa.

[§] As student from INTERCAMPUS and Intercambio Académico UNAM program exchange. Present address: Instituto de Investigaciones Químicas, Departamento de Bioorganica, Sevilla, Spain.

^{||} Universidad Autónoma del Estado de Hidalgo.

The intermolecular interactions and the nature of the ligand are two important factors in these molecular assemblies. It has been shown that redox behavior of these complexes depends on the nature of the ligands, and there is a correlation between their spectroscopic properties and Ru^{II}/Ru^{III} redox potential.^{9–13}

On the other hand, complexes of pdto with Cu(II), Cu(I), Pt(II), Pd(II), Ni(II), Ru(II), Co(II), and Hg(II) have been reported in the literature.^{14–30} In all the complexes, the ligand 1,8-bis(2-pyridyl)-3,6-dithiooctane, pdto (Figure 1), presents a high flexibility toward the preferential geometry of the central atom. Additionally, interactions of pdto complexes with cyclodextrines³¹ and DNA³² have been demonstrated

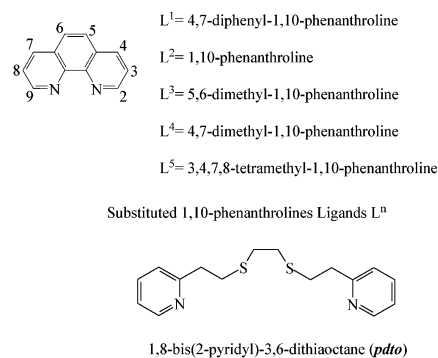


Figure 1. Structure of ligand 1,8-bis(2-pyridyl)-3,6-dithiooctane (pdto) and the substituted 1,10-phenanthrolines used for the synthesis of complexes 3–5.

- (1) Friedman, A. E.; Chambron J.-C.; Sauvague, J. P.; Turro, N. J.; Barton, J. K. *J. Am. Chem. Soc.* **1990**, *112*, 4960–4962.
- (2) Jenkis, Y.; Friedman, A. E.; Turro, N. J.; Barton, J. K. *Biochemistry* **1992**, *31*, 10809–10816.
- (3) Holmlin, R. E.; Stemp, E. D. A.; Barton J. K. *Inorg. Chem.* **1998**, *37*, 29–34.
- (4) Li, L.; Szamacinski, H.; Lakowicz, J. R. *Biospectroscopy* **1997**, *3*, 155–159.
- (5) Li, L.; Szamacinski, H.; Lakowicz, J. R. *Anal. Biochem.* **1997**, *244*, 80–85.
- (6) Terpetsching, E.; Szamacinski, H.; Lakowicz, J. R. *Anal. Biochem.* **1995**, *227*, 140–147.
- (7) Youn, H.; Terpetsching, E.; Szamacinski, H.; Lakowicz, J. R. *Anal. Biochem.* **1995**, *232*, 24–30.
- (8) Murtaza, Z.; Chang, Q.; Rao, G.; Lin, H.; Lakowicz, J. R. *Anal. Biochem.* **1997**, *247*, 216–222.
- (9) Lever, A. B. P. *Inorg. Chem.* **1990**, *29*, 1271–1285.
- (10) Masui, H.; Lever, A. B. P.; Dodsworth, E. S. *Inorg. Chem.* **1993**, *32*, 258–267.
- (11) Vlcek, A. A.; Dodsworth, E. S.; Pierro, W. J.; Lever, A. B. P. *Inorg. Chem.* **1995**, *34*, 1906–1913.
- (12) Doveloglou, A.; Adeyemi, A. S.; Meyer, T. J. *Inorg. Chem.* **1996**, *35*, 5, 4120–4127 and references therein.
- (13) Juris, A.; Balzani, V.; Barigelletti, F.; Campagna, S.; Belser, P.; Zelewsky, A. *Coord. Chem. Rev.* **1998**, *84*, 85–277.
- (14) Goodwin, H. A.; Lions, F. *J. Am. Chem. Soc.* **1960**, *82*, 5013–5023.
- (15) Worrell, J. H.; Genova, J. J.; Dubois, T. D. *J. Inorg. Nucl. Chem.* **1978**, *40*, 441–446.
- (16) Amundsen, A. R.; Whelan, J.; Bosnich, B. *J. Am. Chem. Soc.* **1977**, *99*, 6730–6739.
- (17) Thompson, M.; Whelan, J.; Zemon, D. J.; Bosnich, B.; Solomon, E. I.; Gray, H. B. *J. Am. Chem. Soc.* **1979**, *101*, 2482–2483.
- (18) Sakaguchi, U.; Addison, A. W. *J. Chem. Soc., Dalton Trans.* **1979**, 600–608.
- (19) Brubaker, G. R.; Brown, J. N.; Yoo, M. K.; Kinsey, R. A.; Kutchan, T. M.; Mottel, E. A. *Inorg. Chem.* **1979**, *18*, 299–302.
- (20) Castineiras, A.; Paredes, M. V.; Hiller, W. *Acta Crystallogr., Sect. C: Cryst. Struct. Commun.* **1984**, *40*, 2078–2079.
- (21) Castineiras, A.; Hiller, W.; Paredes, M. V.; Sordo, J.; Strähle, J. *Acta Crystallogr., Sect. A: Found. Crystallogr.* **1984**, *40*, C302.
- (22) Castineiras, A.; Hiller, W.; Paredes, M. V.; Sordo, J.; Strähle, J. *Acta Crystallogr., Sect. C: Cryst. Struct. Commun.* **1985**, *41*, 41.
- (23) Humphery, D. G.; Fallon, G. D.; Murray, K. S. *J. Chem. Soc., Chem. Commun.* **1988**, 1356–1361.
- (24) Castineiras, A.; Diaz, G.; Florencio, F.; García-Blanco, S.; Martínez-Carrera, S. *J. Cristallogr. Spectrosc. Res.* **1988**, *18*, 395–401.
- (25) Castineiras, A.; Diaz, G.; Florencio, F.; García-Blanco, S.; Martínez-Carrera, S. *Z. Anorg. Allg. Chem.* **1988**, *101*, 567.
- (26) Bermejo, E.; Castineiras, A.; Domínguez, A. R.; Strähle, J.; Hiller, W. *Acta Crystallogr., Sect. C* **1993**, *C49*, 324.
- (27) Pavlishchuk, V. V.; Koltikov, S. V.; Michael, E. S.; Prushan, J.; Addison, A. W. *Inorg. Chim. Acta* **1998**, *278*, 217–222.
- (28) Bermejo, E.; Castineiras, A.; Domínguez, A. R.; Strähle, J.; Hiller, W. *Acta Crystallogr., Sect. C* **1993**, *49*, 1918–1920.
- (29) Davies, K. M. Whyte, K. D. Gilbert, A. H. *Inorg. Chim. Acta* **1990**, *177*, 121–126.
- (30) Davies, K. M. Whyte, K. D. Liebermann, J. Mahr, J. A. *Polyhedron* **1991**, *10*, 1647–1651.
- (31) Sivagnanam, U.; Palaniandavar, M. *J. Chem. Soc., Dalton Trans.* **1996**, 2609–2615.
- (32) Mahadevan, S.; Palaniandavar, M. *Inorg. Chim. Acta* **1997**, *254*, 291–302.
- (33) La Placa, S. J.; Ibers, J. A. *Inorg. Chem.* **1965**, *4*, 778–783.

by electrochemical methods. The flexibility of pdto, the photochemical properties of Ru(II) polypyridine complexes, and the possible intermolecular interactions with biomolecules direct us to synthesize complexes capable of forming macromolecular assemblies as new prospective probes for biochemistry and clinical diagnosis.

This work presents the synthesis and characterization of different coordination compounds of Ru(II) with pdto and different substituted 1,10-phenanthrolines, [Ru(pdto)Lⁿ]₂Cl₂, where n = 1–5 (Figure 1). Several substituted phenanthrolines were used to obtain complexes 3–7 in order to modify electrochemical and possibly photochemical properties. Electrochemical studies of these complexes were performed in order to understand the influence of the nature of ligands in the redox behavior. Due to the easy replacement of chloride and triphenylphosphine ligands (in cis position), the complex [Ru(pdto)(PPh₃)Cl]₂Cl (1) was used as the starting material for the complexes 3–7. This substitution can be observed using NMR, X-ray diffraction, and conductivity measurements. Additionally electrochemical studies were also used as a supplementary technique to demonstrate this fact.

Experimental Section

Chemicals and Reagents. The ligands 4,7-diphenyl-1,10-phenanthroline (L¹), 1,10-phenanthroline (L²), 5,6-dimethyl-1,10-phenanthroline (L³), 4,7-dimethyl-1,10-phenanthroline (L⁴), and 3,4,7,8-tetramethyl-1,10-phenanthroline (L⁵) and all chemicals and solvents for synthesis and characterization were purchased from Aldrich Chemical Co. and used without further purification.

1,8-Bis(2-pyridyl)-3,6-dithiooctane (pdto) was prepared by the method described by Goodwin and Lions.¹⁴ Yield: 70%. Elemental anal. Calcd for C₁₆H₂₀N₂S₂: C, 63.1; H, 6.6; N, 9.2; S, 20.1. Found: C, 63.1; H, 6.2; N, 9.7; S, 20.5.

Dichlorotris(triphenylphosphine) ruthenium(II) [RuCl₂(PPh₃)₃] was prepared by a modification of the reported technique³³ as follows: RuCl₃(H₂O)₃ (1.00 g, 3.81 mmol) was dissolved in 50 mL of methanol, and a 6-fold excess of triphenylphosphine (6.00 g, 22.86 mmol) was added. The solution was heated under reflux for 4 h. A brown solid was filtered and washed several times with diethyl ether to eliminate the excess of triphenylphosphine. Yield: 94%. Elemental anal. Calcd for C₅₄H₄₅RuCl₂: C, 67.6; H, 4.7. Found: C, 67.0; H, 4.9.

Chloro triphenylphosphine 1,8-bis(2-pyridyl)-3,6-dithiaoctane ruthenium(II) chloride, [Ru(pdto)Cl(PPh₃)Cl] (1). Reagent grade pdto (0.304 g, 1.0 mmol) was added to a solution of [Ru(PPh₃)₃-Cl₂] (0.957 g, 1.0 mmol) previously dissolved in 50 mL of methanol. The reaction mixture was heated under reflux for 3 h, cooled, and concentrated, and a yellow powder appeared. This powder was washed several times with diethyl ether to eliminate the excess of triphenylphosphine and was then recrystallized with dichloromethane, from which a yellow crystalline solid (**1**) was filtered off. Yield: 90%. Elemental anal. Calcd for C₃₄H₃₅N₂S₂PRuCl₂: C, 55.3; H, 4.8; N, 3.8; S, 8.7. Found: C, 55.1; H, 4.8; N, 3.7; S, 8.5. FAB(+): *m/z* 703 [Ru(pdto)Cl(PPh₃)]⁺. $\Lambda = 125.2 \text{ S cm}^2 \text{ mol}^{-1}$.

Chloro triphenylphosphine 1,8-bis(2-pyridyl)-3,6-dithiaoctane ruthenium(II) hexafluorophosphate [Ru(pdto)Cl(PPh₃)PF₆] (1a). 0.031 mmol (0.0203 g) of **1** was dissolved in 25 mL of methanol and then treated with equimolecular quantities of ammonium hexafluorophosphate (0.0044 g) to induce crystallization. Suitable yellow crystals for X-ray diffraction were obtained. Yield: 80%. Elemental anal. Calcd for C₃₄H₃₅N₂S₂P₂RuClF₆: C, 48.1; H, 4.2; N, 3.3; S, 7.5. Found: C, 48.8; H, 4.2; N, 3.6; S, 7.5. FAB(+): *m/z* 703 [Ru(pdto)Cl(PPh₃)]⁺.

Bis(acetonitrile)1,8-bis(2-pyridyl)-3,6-dithiaoctane ruthenium(II) chloride, [Ru(pdto)(CH₃CN)₂]Cl₂ (2). **1** (0.0556 g, 0.1 mmol) was added to 50 mL of acetonitrile. The mixture was heated under reflux for 4 h, cooled, and concentrated to 5 mL, and finally, by addition of 20 mL of diethyl ether, an orange precipitate was isolated. Suitable crystals for X-ray analysis were obtained from acetonitrile. Yield: 95%. Elemental anal. Calcd for C₂₀H₂₆N₄S₂-RuCl₂: C, 43.0; H, 4.7; N, 10.0; S, 11.5. Found: C, 43.1; H, 4.7; N, 10.1; S, 11.5. $\Lambda = 250 \text{ S cm}^2 \text{ mol}^{-1}$.

Synthesis of the Substituted Phenanthroline pdto Ru(II) Complexes. All of these coordination complexes were prepared following the next procedure: 0.1 mmol of L^{*n*} was added to 0.0738 g (0.1 mmol) of [Ru(pdto)(PPh₃)Cl]Cl, previously dissolved in 50 mL of methanol. The mixture was heated under reflux for 3 h, cooled, and concentrated to 5 mL, and finally, by addition of 20 mL of ether, in all cases an orange precipitate was isolated.

[Ru(pdto)(L¹)]Cl₂·4H₂O (3). [Ru(pdto)(4,7-diphenyl-1,10-phenanthroline)]Cl₂·4H₂O. Yield: 75%. Elemental anal. Calcd for C₄₀H₄₄O₄N₄S₂RuCl₂: C, 54.5; H, 4.9; N, 6.4; S, 7.3. Found: C, 54.8; H, 4.9; N, 6.3; S, 7.4. $\Lambda = 170 \text{ S cm}^2 \text{ mol}^{-1}$

[Ru(pdto)(L²)]Cl₂·5H₂O (4). [Ru(pdto)(1,10-phenanthroline)]Cl₂·5H₂O. Yield: 94%. Elemental anal. Calcd for C₂₈H₃₈O₅N₄S₂-RuCl₂: C, 45.6; H, 5.1; N, 7.5; S, 8.6. Found: C, 45.2; H 5.1; N, 7.5; S, 8.5. $\Lambda = 275 \text{ S cm}^2 \text{ mol}^{-1}$. Suitable crystals for X-ray analysis for this compound were obtained from a mixture of acetonitrile–water (6:1).

[Ru(pdto)(L³)]Cl₂·5H₂O (5). [Ru(pdto)(5,6-dimethyl-1,10-phenanthroline)]Cl₂·5H₂O. Yield: 65%. Elemental anal. Calcd for C₃₀H₄₂O₅N₄S₂RuCl₂: C, 46.4; H, 5.5; N, 7.2; S, 8.3. Found: C, 46.0; H 5.3; N, 7.2; S, 8.5. $\Lambda = 273 \text{ S cm}^2 \text{ mol}^{-1}$

[Ru(pdto)(L⁴)]Cl₂·3H₂O (6). [Ru(pdto)(4,7-dimethyl-1,10-phenanthroline)]Cl₂·3H₂O. Yield: 70%. Elemental anal. Calcd for C₃₀H₃₈O₃N₄S₂RuCl₂: C, 45.6; H, 5.1; N, 7.5; S, 8.6. Found: C, 45.2; H, 5.1; N, 7.5; S, 8.5. $\Lambda = 243 \text{ S cm}^2 \text{ mol}^{-1}$

[Ru(pdto)(L⁵)]Cl₂·4H₂O (7). [Ru(pdto)(3,4,7,8-tetramethyl-1,10-phenanthroline)]Cl₂·4H₂O. Yield: 91%. Elemental anal. Calcd for C₃₂H₄₄O₄N₄S₂RuCl₂: C, 49.0; H, 5.7; N, 7.1; S, 8.2. Found: C, 49.1; H, 5.6; N, 7.0; S, 8.1. $\Lambda = 252 \text{ S cm}^2 \text{ mol}^{-1}$

Physical Measurements. Fissons Instruments analyzer model EA 1108 was used for elemental analysis determination, using a sulfanilamide standard. Mass spectra were obtained in a JEOL

Table 1. Crystal Data Collection for Complexes

	1a	2	4
empirical formula	C ₃₄ H ₃₅ ClF ₆ N ₂ -O _{0.5} P ₂ RuS ₂	C ₂₀ H ₂₈ Cl ₂ N ₄ -OCl ₂ RuS ₂	C ₂₈ H ₂₈ Cl ₂ N ₄ -O _{3.5} RuS ₂
fw	852.22	576.55	712.63
temp, K	291(2)	294(2)	293(2)
wavelength, Å	0.71073	0.71073	0.71073
cryst syst	monoclinic	monoclinic	monoclinic
space group	<i>P</i> 2 ₁ / <i>c</i>	<i>C</i> 2/ <i>c</i>	<i>I</i> 2/ <i>a</i>
lattice params			
<i>a</i> , Å	10.9879(7)	13.601(1)	22.689(1)
<i>b</i> , Å	23.126(2)	16.312(1)	11.922(1)
<i>c</i> , Å	14.470(1)	11.326(1)	25.835(2)
β , deg	93.710(2)	102.16(1)	109.06(1)
vol, Å ³	3669.3(4)	2456.5(3)	6605(3)
<i>Z</i>	4	4	8
density (calcd), mg/m ³	1.543	1.559	1.433
abs coeff, mm ⁻¹	0.760	1.045	0.798
final <i>R</i> indices	<i>R</i> 1 = 0.0561	<i>R</i> 1 = 0.0388	<i>R</i> 1 = 0.0448
[<i>I</i> > 2 σ (<i>I</i>)]	w <i>R</i> 2 = 0.0831	w <i>R</i> 2 = 0.1263	w <i>R</i> 2 = 0.1293
<i>R</i> indices	<i>R</i> 1 = 0.1661	<i>R</i> 1 = 0.0402	<i>R</i> 1 = 0.0792
(all data)	w <i>R</i> 2 = 0.1083	w <i>R</i> 2 = 0.1270	w <i>R</i> 2 = 0.1418

SX102A mass spectrometer with a matrix of nitrobenzyl alcohol and dissolved in CH₃CN. A VARIAN Unity Inova spectrometer was used to record all NMR spectra, ¹H (300 MHz), ¹³C (75.5 MHz), and ³¹P spectra (121 MHz); TMS and H₃PO₄ were used as reference, and acetonitrile-*d*₃ was used as solvent. A Hewlett-Packard 5484A diode array spectrophotometer was used to acquire UV–vis spectra, using acetonitrile as solvent. Conductivities were measured with a SUNTEX model SC170 conductivity meter. The conductivity data were obtained at sample concentrations of ca. 1 × 10⁻⁴ M in acetonitrile solutions at 25.0(±0.5) °C. All electrochemical measurements were performed in acetonitrile (HPLC grade) solution containing 0.1 M tetra-*N*-butylammonium tetrafluoroborate (TBATFB) as supporting electrolyte. A potentiostat/galvanostat EG&G PARC model 273 controlled by PC software was used. A typical three-electrode array was employed for all electrochemical measurements: platinum disk as working electrode, platinum wire as counter electrode, and a pseudo reference electrode of silver wire immersed in an acetonitrile solution with 0.1 M tetra-*N*-butylammonium chloride (TBACl). All solutions were bubbled with nitrogen prior each measurement. All voltammograms were initiated from open circuit potential (*E*_{ocp}), and the scan potential was obtained in both positive and negative directions. All the potentials were reported versus the couple Fc/Fc⁺ according to IUPAC convention.³⁴

X-ray Analysis of Compounds 1a, 2, and 4. X-ray diffraction data were collected with a Bruker 6000 CCD area detector diffractometer and analyzed using monochromated Mo K α X-ray radiation ($\lambda = 0.71073 \text{ \AA}$). The crystal dimensions of the analyzed crystals **1a**, **2**, and **4** were respectively 0.25 × 0.18 × 0.11 mm, 0.4 × 0.25 × 0.2 mm, and 0.3 × 0.2 × 0.19 mm. Unit cell parameters along with data collection and refinement details for compounds **1a**, **2**, and **4** are listed in Table 1. All structures were solved by Patterson methods using SHELXS 97-2.³⁵ Least-squares refinement based on *F*² was carried out by full-matrix method of SHELXL-97-2.³⁶ All non-hydrogen atoms were refined with anisotropic thermal parameters. Location of hydrogen atoms was generated geometrically and included in the refinement with an

(34) Gritzner, G.; Küta J., *Pure Appl. Chem.* **1984**, *4*, 461–466.

(35) Sheldrick, G. M. *SHELXS-97-2. Program for Crystal Structure Refinement*; University of Göttingen: Göttingen, Germany, 1997.

(36) Sheldrick, G. M. *SHELXL-97-2. Program for Crystal Structure Refinement*; University of Göttingen: Göttingen, Germany, 1997.

Table 2. Selected Bond Lengths (Å) and Angles (deg) for **1a**

Cl(1)–Ru(1)	2.441(2)	P(1)–Ru(1)	2.398(2)
N(1)–Ru(1)	2.154(5)	Ru(1)–S(1)	2.292(2)
N(2)–Ru(1)	2.138(6)	Ru(1)–S(2)	2.366(2)
N(2)–Ru(1)–N(1)	172.8(2)	N(1)–Ru(1)–P(1)	92.8(2)
N(2)–Ru(1)–S(1)	92.4(2)	S(1)–Ru(1)–P(1)	98.0(6)
N(1)–Ru(1)–S(1)	84.9(2)	S(2)–Ru(1)–P(1)	173.8(1)
N(2)–Ru(1)–S(2)	82.9(2)	N(2)–Ru(1)–Cl(1)	89.2(2)
N(1)–Ru(1)–S(2)	90.3(2)	N(1)–Ru(1)–Cl(1)	93.0(2)
S(1)–Ru(1)–S(2)	87.6(7)	S(2)–Ru(1)–Cl(1)	89.1(1)
N(2)–Ru(1)–P(1)	94.2(2)	P(1)–Ru(1)–Cl(1)	85.5(1)

Table 3. Selected Bond Lengths (Å) and Angles (deg) for **2^a**

Ru(1)–N(2)#1	2.098(4)	Ru(1)–S(1)	2.300(1)
Ru(1)–N(1)#1	2.136(4)	Ru(1)–S(1)#1	2.300(1)
N(2)–Ru(1)–N(2)#1	83.5(2)	N(2)#1–Ru(1)–S(1)	94.5(1)
N(2)–Ru(1)–N(1)	90.9(1)	N(1)–Ru(1)–S(1)	93.5(1)
N(2)–Ru(1)–N(1)#1	92.2(1)	N(1)#1–Ru(1)–S(1)	83.5(1)
N(1)–Ru(1)–N(1)#1	175.8(2)	N(1)–Ru(1)–S(1)#1	83.4(1)
N(2)–Ru(1)–S(1)	175.2(1)	S(1)–Ru(1)–S(1)#1	87.9(6)

^a Symmetry transformations used to generate equivalent atoms: #1 $-x + 1, y, -z + 3/2$.

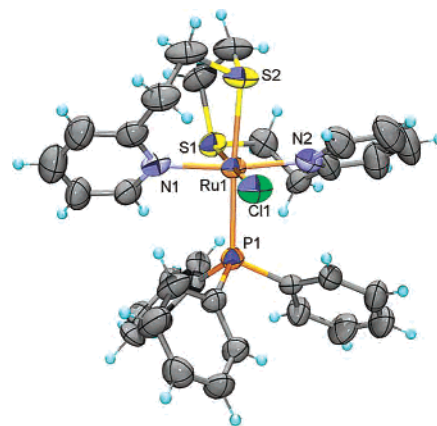
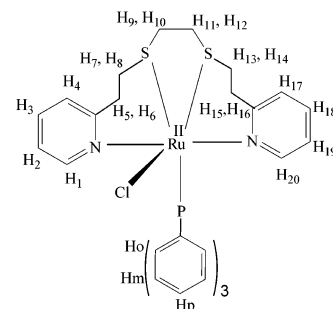
Table 4. Bond Lengths (Å) and Angles (deg) for **4**

Ru(1)–N(4)	2.104(4)	Ru(1)–N(1)	2.142(4)
Ru(1)–N(3)	2.112(4)	Ru(1)–S(1)	2.312(2)
Ru(1)–N(2)	2.143(4)	Ru(1)–S(2)	2.319(1)
N(4)–Ru(1)–N(3)	78.1(2)	N(1)–Ru(1)–S(1)	93.6(1)
N(4)–Ru(1)–N(1)	90.6(2)	N(2)–Ru(1)–S(1)	85.5(1)
N(3)–Ru(1)–N(1)	89.1(2)	N(4)–Ru(1)–S(2)	175.0(1)
N(4)–Ru(1)–N(2)	90.8(2)	N(3)–Ru(1)–S(2)	98.1(1)
N(3)–Ru(1)–N(2)	92.0(2)	N(1)–Ru(1)–S(2)	86.0(1)
N(1)–Ru(1)–N(2)	178.4(2)	N(2)–Ru(1)–S(2)	92.6(1)
N(4)–Ru(1)–S(1)	96.7(1)	S(1)–Ru(1)–S(2)	87.3(1)
N(3)–Ru(1)–S(1)	174.1(1)		

isotropic fixed thermal parameter using a “riding” model. Neutral atom scattering factors and anomalous dispersion corrections were taken from *International Tables for Crystallography*.³⁷ Selected bond lengths and angles of the compounds **1a**, **2**, and **4** are listed in Tables 2, 3, and 4, respectively; molecular structure drawings were generated using ORTEP3 for Windows.³⁸

Results and Discussion

Characterization of the Starting Compound. Elemental analysis and conductometric measurement are in agreement with the proposed formulas for **1** and **1a**. The FAB mass spectrum peak at (+) m/z 703 corresponding to the fragment $[\text{Ru}(\text{pdto})\text{Cl}(\text{PPh}_3)]^+$ was detected for both complexes. The molecular structure of **1a** has been determined by X-ray diffraction and is shown in Figure 2. The complex has a distorted octahedral geometry around the ruthenium(II) with trans-oriented nitrogen ligand atoms [N(1)–Ru(1)–N(2) 172.8(2)°] from the pdto; two cis configurations are also presented, the first between chloride and triphenylphosphine [Cl(1)–Ru(1)–P(1) 85.5(1)°] and the second between the sulfur atoms from the pdto [S(1)–Ru(1)–S(2) 87.6(1)°]. The Ru(1)–S(2) bond trans to P(1) is elongated (2.366(2) Å) compared to Ru(1)–S(1) trans to Cl(1) (2.292(2) Å) due to

**Figure 2.** ORTEP diagram showing the molecular structure of the cation $[\text{Ru}(\text{pdto})\text{Cl}(\text{PPh}_3)]^+$ (**1a**) with 50% probability displacement ellipsoids.**Table 5.** ¹H NMR Spectroscopic Data for Complex **1^a**

$\delta\text{H}_1 = 9.86$ dd(1); $\delta\text{H}_2 = 7.25$ ddd(1); $\delta\text{H}_3 = 7.65$ ddd(1); $\delta\text{H}_4 = 7.30$ dd(1); $\delta\text{H}_{5,6} = 4.80$ td(1), 3.18 ddd(1); $\delta\text{H}_{7,8} = 1.95$ td(1), 3.50 dd(1); $\delta\text{H}_{9,10} = 3.05$ dd(1), 1.84 ddd(1); $\delta\text{H}_{11,12} = 2.74$ dd(1), 1.84 ddd(1); $\delta\text{H}_{13,14} = 1.95$ ddd(1), 2.82 td(1); $\delta\text{H}_{15,16} = 3.32$ ddd(1), 2.50 td(1); $\delta\text{H}_{17} = 6.91$ dd(1); $\delta\text{H}_{18} = 7.59$ ddd(1); $\delta\text{H}_{19} = 6.55$ ddd(1); $\delta\text{H}_{20} = 8.74$ dd(1)
$J_{1-2} = 6.29$; $J_{1-3} = 1.50$; $J_{2-3} = 7.49$; $J_{2-4} = 1.50$; $J_{3-4} = 7.79$; $J_{5-7} = 15.88$; $J_{5-8} = 15.88$; $J_{5-6} = 2.09$; $J_{6-7} = 15.28$; $J_{6-8} = 4.79$; $J_{7-8} = 2.09$; $J_{9-10} = 2.08$; $J_{9-12} = 4.79$; $J_{10-11} = 10.19$; $J_{10-12} = 4.79$; $J_{11-12} = 2.08$; $J_{13-14} = 4.49$; $J_{13-16} = 16.18$; $J_{13-15} = 7.49$; $J_{16-14} = 14.98$; $J_{16-15} = 2.10$; $J_{14-15} = 12.59$; $J_{18-20} = 1.50$; $J_{18-19} = 7.19$; $J_{19-20} = 5.69$; $J_{17-19} = 1.50$; $J_{17-18} = 7.79$
$\text{H}_{\text{o,m,p}} = 6.62, 7.20, 7.50$ (broad signals)

^a δ , multiplicity, (integration), J/Hz .

the trans influence of the coordinated triphenylphosphine ligand. The bond lengths Ru(1)–N(1) (2.154(1) Å) and Ru(1)–N(2) (2.138(1) Å) are fairly equivalent.

The ¹H NMR spectrum for **1** at 298 K was obtained in acetonitrile-*d*₃. Considering that there are no significant changes in the molecular structure in the solid state and solution, the unequivocal assignment was achieved with a 2D correlated COSY experiment; hydrogen assignments are listed in Table 5. The high chemical shift value for H₁ ($\delta = 9.86$ ppm) compared to the H₂₀ value ($\delta = 8.74$ ppm) and their magnetic inequivalence are attributed to the fact that H₁ is closer than H₂₀ to the chloride atom. The broad signals in ¹H NMR spectrum can be attributed to the restricted rotation of the aromatic groups of triphenylphosphine: H_o, H_m, H_p.

The ³¹P NMR spectrum shows only one signal at $\delta = 40.01$ ppm, which suggests a unique species of phosphorus atom coordinated to Ru(II). The ¹H and ³¹P NMR spectra of complexes **1** and **1a** are essentially the same.

(37) Wilson, A. J. C., Ed. *International Tables for Crystallography*; Kluwer Academic Publishers: Dordrecht, The Netherlands, 1995; Vol. C, Table 4.2.4.2, p 193.

(38) Farrugia, L. ORTEP3 for Windows. *J. Appl. Crystallogr.* **1997**, *30*, 565.

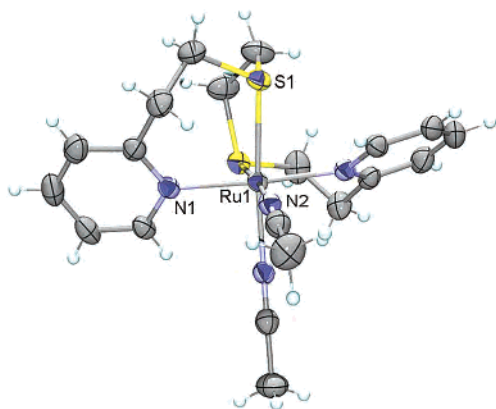


Figure 3. ORTEP diagram showing the molecular structure of the cation $[\text{Ru}(\text{pdto})(\text{CH}_3\text{CN})_2]^{2+}$ (**2**) with 50% probability displacement ellipsoids.

Temperature ^1H and ^{31}P NMR and Conductivity Studies of **1.** A ^1H NMR study in acetonitrile- d_3 was performed at several temperatures, from 223 to 353 K, with an increment of 10 K in order to obtain information about the stability of compound **1**. In experiments from 223 to 293 K, a broadening of the signals corresponding to aromatic protons is observed, this is due to the restricted rotation of the phenyl protons in the triphenylphosphine coordinated to the Ru(II) atom. When the temperature was raised to 313 K, three new signals appeared, at 9.65, 9.12, and 7.74 ppm, while the initial pyridinic aromatic signals for H_1 – H_4 and H_{17} – H_{20} decreased. This phenomenon persisted until a temperature of 353 K was reached, when the signal disappeared.

As pointed out above, the ^{31}P NMR spectrum of compound **1** presents only one signal P_1 ($\delta = 40.01$ ppm) at 293 K. When the measurement was performed at 303 K, a negligible shift in the signal P_1 ($\delta = 39.96$ ppm) and the appearance of a new signal P_2 at 0.34 ppm were observed. At 353 K the signal P_2 shifted to 1.25 ppm and the original signal P_1 disappeared. The ^{31}P NMR spectra of noncoordinated triphenylphosphine at 303 K shows a signal at 0.06 ppm, and when the sample was warmed to 353 K, a signal at 1.26 ppm was detected. The above results clearly show that in compound **1** the triphenylphosphine is substituted by acetonitrile as the temperature is increased.

In a polar solvent such as acetonitrile the coordinated chloride ligand should also be exchanged; this suggestion was confirmed with a conductometric experiment. The conductivity of a 10^{-3} M solution of **1** in acetonitrile at 298 K was $\kappa = 136.5 \mu\text{S cm}^{-1}$ ($\Lambda = 125.2 \text{ S cm}^2 \text{ mol}^{-1}$), corresponding to a 1:1 electrolyte. When the solution was warmed to 353 K and later on was cooled to room temperature, the conductivity value increased to $\kappa = 2030 \mu\text{S cm}^{-1}$. From the above solution yellow crystals were recovered, and the structure was determined by X-ray diffraction techniques; two acetonitrile molecules are coordinated to Ru(II), corresponding to the compound $[\text{Ru}(\text{pdto})(\text{CH}_3\text{CN})_2]\text{Cl}_2$ (**2**), see Figure 3. The complex has a distorted octahedral geometry around the ruthenium(II) with trans-oriented nitrogen ligand atoms [$\text{N}(1)\#\text{1}-\text{Ru}(1)-\text{N}(1)$, $175.8(2)^\circ$] from the pdto and two molecules of acetonitrile in cis

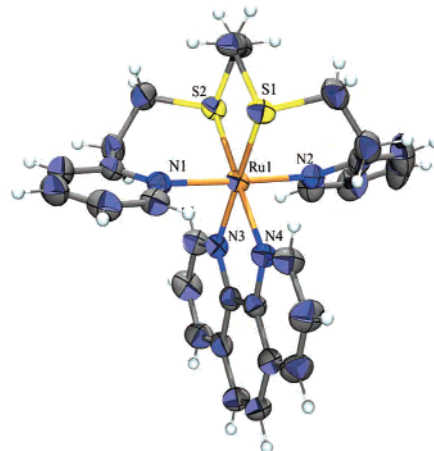


Figure 4. ORTEP diagram showing the molecular structure of the cation $[\text{Ru}(\text{pdto})(1,10\text{-phenanthroline})]^{2+}$ (**4**) with 50% probability displacement ellipsoids.

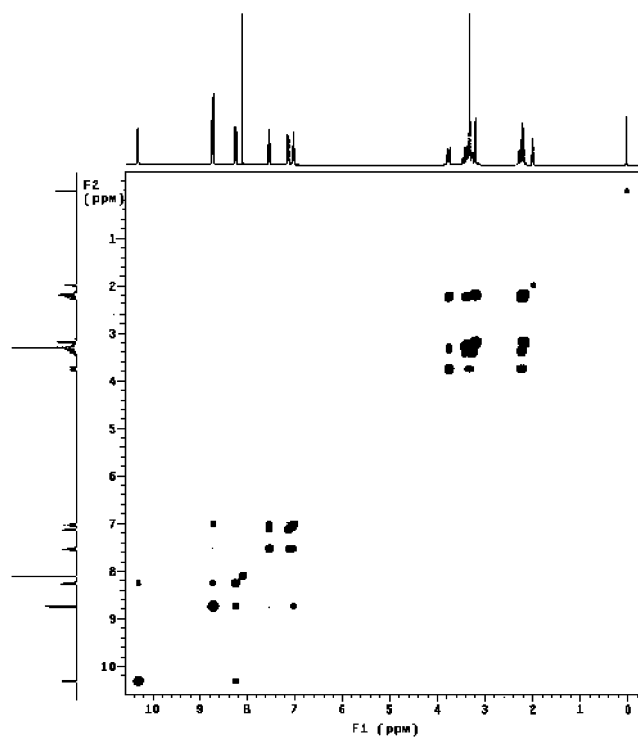


Figure 5. COSY experiment for **4**, recorded at 300 MHz. Acetonitrile- d_3 was employed as solvent.

array [$\text{N}(2)-\text{Ru}(1)-\text{N}(2)\#\text{1}$, $83.5(2)^\circ$]; sulfur atoms are also in a cis configuration [$\text{S}(1)-\text{Ru}(1)-\text{S}(1)\#\text{1}$, $87.9(1)^\circ$].

In order to fully characterize **2**, the synthesis from **1** in acetonitrile was done, and the solid obtained from this synthesis was characterized. ^1H NMR spectrum of compound **2** in acetonitrile was also obtained. The NMR spectra of compound **2** presents three signals with the same chemical shift values as those observed in the ^1H NMR spectra for compound **1** from 313 to 353 K. The conductivity of a 10^{-3} M solution, at 298 K in acetonitrile solution for this compound, corresponds to a 1:2 electrolyte, $\kappa = 2050 \mu\text{S cm}^{-1}$, $\Lambda = 250 \text{ S cm}^2 \text{ mol}^{-1}$.

From this discussion, it is feasible to conclude that, in polar solvents, both ligands (chloride and triphenylphosphine) are easily substituted by solvent molecules.

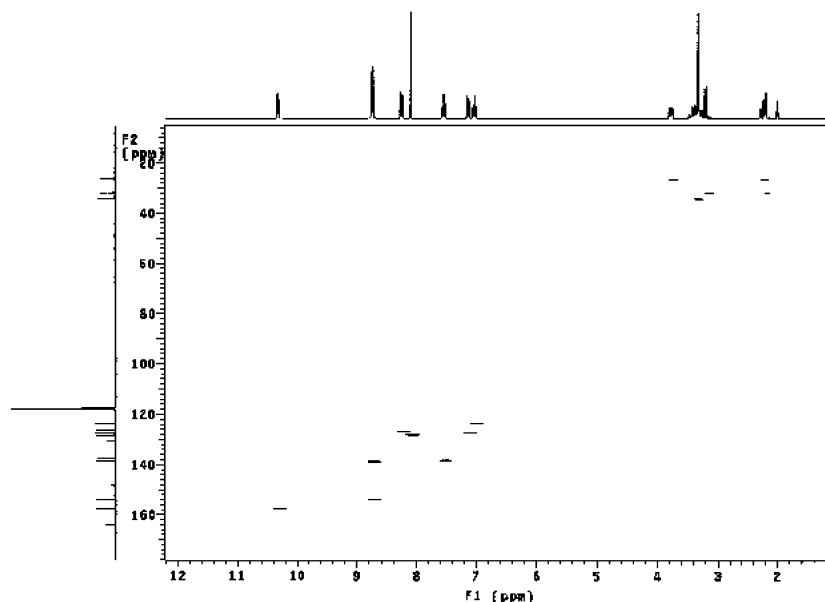


Figure 6. HETCOR experiment for **4**, recorded at 300 MHz. Acetonitrile- d_3 was employed as solvent.

Characterization of the Substituted Phenanthroline pdto Ru(II) Complexes. Conductivity measurements and elemental analyses for all the compounds correspond to the proposed formulas (**3–7**).

The crystal structure of molecule **4** obtained by X-ray diffraction is shown in Figure 4. This complex has a slightly distorted octahedral geometry around the ruthenium(II) with the pdto nitrogen atoms [N(1)–Ru(1)–N(2), 178.4(2)°] in trans position and the two nitrogen atoms of 1,10-phenanthroline [N(3)–Ru(1)–N(4), 78.1(2)°] in a cis arrangement; the sulfur atoms are also in a cis configuration [S(1)–Ru(1)–S(2), 87.3(1)°].

^1H and ^{13}C NMR spectra for **4** at 298 K in acetonitrile- d_3 were acquired. Assuming again that there are no significant changes in the molecular structure going from solid state to solution, unequivocal ^1H and ^{13}C NMR assignments were achieved by 2D correlated COSY (Figure 5) and HETCOR (Figure 6) experiments, ^1H and ^{13}C assignments of the molecules (**3–5**) are listed in Tables 6 and 7. NMR spectra for the compounds (**3**, **5**, **6**, and **7**) are very similar to the spectrum of **4**, excluding the signals due to the substituents of the corresponding 1,10-phenanthrolines; the signals for ligand pdto are basically the same. The magnetic equivalence of hydrogen and carbon in the coordinated pdto ligand, for all the compounds, suggest a trans configuration of the pyridine rings.

Table 8 shows the selected electronic spectra absorption data for compounds **3–7**. The spectra for all complexes are analogous, and all show six bands (3 MLCT, 2 LC, and 1 MC transition bands). The strongest absorption band in the UV region can be assigned as an intraligand LC ($\pi \rightarrow \pi^*$) transition. Alternatively the absorption band in the visible region near 400 nm can be assigned to a metal-to-ligand charge-transfer (MLCT) transition (due to (phenanthroline), by analogy to spectral assignments of similar absorption in the compounds $[\text{Ru}^{\text{II}}(\text{phen})_3]^{2+}$).

Electrochemical Studies of the Starting Material Compound 1. Cyclic voltammetric experiments for compound **1**

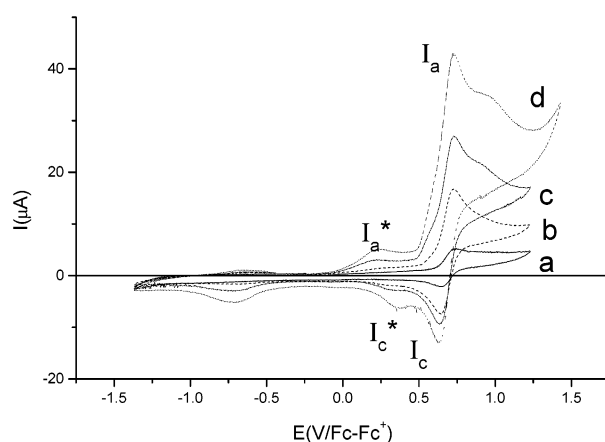
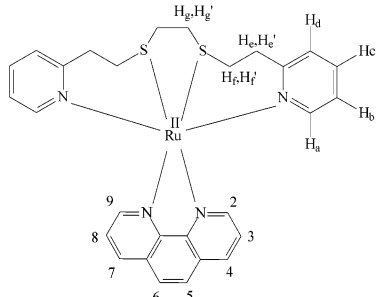


Figure 7. Cyclic voltammograms of compound **1** in the presence of 0.1 M TBABF $_4$ in acetonitrile. The scan potential was initiated from E_{ocp} to positive direction. Scan rate: 200 mV s^{-1} . Each experiment was acquired at a different concentration of **1**: (a) 0.365, (b) 1.422, (c) 2.01, and (d) 2.70 mM.

at different concentrations were performed (Figure 7). When the potential scan was initiated in the positive direction, in the lowest concentration of **1** (Figure 7a), an anodic oxidation signal (I_a) and a reduction signal (I_c) (after the scan potential was inverted) are presented. Additionally, a second oxidation signal (I_a^*) and a reduction signal (I_c^*), see Figure 7c,d, appear when the concentration of **1** increases.

To obtain information on the electrochemical process, controlled potential coulometry and spectroelectrochemical studies were also performed. Two electrons per molecule were determined by coulometry at a potential more positive than the peak I_a (1.13 V/Fc–Fc $^+$); a change in solution color from yellow to green was observed. Cyclic voltammograms were recorded before and after electrolysis. In both cases, the scan potential was initiated from the open circuit potential, $E_{\text{ocp}} = -0.240$ V/Fc–Fc $^+$ (before electrolysis) and $E_{\text{ocp}} = 0.633$ V/Fc–Fc $^+$ (after electrolysis). From the cyclic voltammogram obtained in the positive direction after the electrolysis, the absence of an oxidation signal suggests the

Table 6. ¹H NMR Spectroscopic Data for Complexes 3–7^a


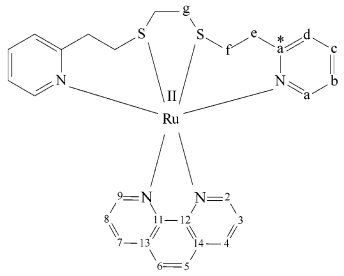
3	$\delta H_a = 8.81$ d(2); $\delta H_b = 7.08$ ddd(2); $\delta H_c = 7.57$ td(2); $\delta H_d = 7.10$ dd(2); $\delta H_{e,e'} = 2.25$ td(2), 3.76 ddd(2); $\delta H_{f,f'} = 3.74$ td(2), 3.29 ddd(2); $\delta H_{g,g'} = 3.18$ d(2), 2.19 d(2); $J_{a-b} = 6.00$; $J_{b-c} = 7.50$; $J_{b-d} = 1.50$; $J_{c-a} = 1.50$; $J_{c-d} = 7.50$; $J_{c-e} = 1.20$; $J_{e-e'} = 2.10$; $J_{e-f} = 12.60$; $J_{e-f'} = 12.60$; $J_{e'-f} = 12.60$; $J_{e'-f'} = 5.10$; $J_{f-f'} = 2.10$; $J_{g-g'} = 9.90$, $\delta H_2 = 10.34$ d(2); $\delta H_3 = 8.16$ d(2); $\delta H_5 = 8.01$ s(2); $\delta_{(4)}C_6H_5 = (7.678-7.592)$ m(12); $J_{2-3} = 5.70$
4	$\delta H_a = 8.73$ d(2); $\delta H_b = 7.02$ ddd(2); $\delta H_c = 7.53$ td(2); $\delta H_d = 7.12$ dd(2); $\delta H_{e,e'} = 2.22$ td(2), 3.75 ddd(2); $\delta H_{f,f'} = 3.40$ td(2), 3.33 ddd(2); $\delta H_{g,g'} = 3.17$ d(2), 2.17 d(2); $J_{a-b} = 6.30$; $J_{b-c} = 7.50$; $J_{b-d} = 1.50$; $J_{c-a} = 1.50$; $J_{c-d} = 7.50$; $J_{c-e} = 1.20$; $J_{e-e'} = 2.10$; $J_{e-f} = 12.90$; $J_{e-f'} = 12.90$; $J_{e'-f} = 12.90$; $J_{e'-f'} = 5.10$; $J_{f-f'} = 2.10$; $J_{g-g'} = 9.60$, $\delta H_2 = 10.32$ d(2); $\delta H_3 = 8.25$ dd(2); $\delta H_4 = 8.73$ d(2); $\delta H_5 = 7.12$ s(2); $J_{2-3} = 4.50$; $J_{3-4} = 8.40$
5	$\delta H_a = 8.72$ dd(2); $\delta H_b = 7.00$ ddd(2); $\delta H_c = 7.44$ td(2); $\delta H_d = 7.11$ dd(2); $\delta H_{e,e'} = 2.22$ td(2), 3.75 ddd(2); $\delta H_{f,f'} = 3.39$ td(2), 3.26 ddd(2); $\delta H_{g,g'} = 3.17$ d(2), 2.17 d(2); $J_{a-b} = 6.90$; $J_{a-c} = 1.20$; $J_{b-c} = 7.50$; $J_{b-d} = 1.50$; $J_{c-d} = 7.50$; $J_{c-e} = 2.10$; $J_{e-e'} = 12.60$; $J_{e-f} = 12.60$; $J_{e-f'} = 12.60$; $J_{e'-f} = 5.10$; $J_{f-f'} = 2.10$; $J_{g-g'} = 9.90$, $\delta H_2 = 10.26$ d(2); $\delta H_3 = 8.23$ dd(2); $\delta H_4 = 8.86$ dd(2); $\delta_{(5)}CH_3 = 2.72$ s(6); $J_{2-3} = 4.20$; $J_{3-4} = 8.70$; $J_{4-1} = 1.20$
6	$\delta H_a = 8.72$ dd(2); $\delta H_b = 7.00$ ddd(2); $\delta H_c = 7.52$ td(2); $\delta H_d = 7.11$ dd(2); $\delta H_{e,e'} = 2.22$ td(2), 3.71 ddd(2); $\delta H_{f,f'} = 3.38$ td(2), 3.28 ddd(2); $\delta H_{g,g'} = 3.15$ d(2), 2.15 d(2); $J_{a-b} = 6.00$; $J_{a-c} = 1.50$; $J_{b-c} = 7.50$; $J_{b-d} = 1.50$; $J_{c-d} = 7.50$; $J_{c-e} = 2.10$; $J_{e-e'} = 12.90$; $J_{e-f} = 12.90$; $J_{e-f'} = 12.90$; $J_{e'-f} = 5.10$; $J_{f-f'} = 2.10$; $J_{g-g'} = 9.90$, $\delta H_2 = 10.13$ d(2); $\delta H_3 = 8.08$ d(2); $\delta H_5 = 8.24$ s(2); $\delta_{(4)}CH_3 = 2.94$ s(6); $J_{2-3} = 5.70$
7	$\delta H_a = 8.72$ dd(2); $\delta H_b = 7.01$ ddd(2); $\delta H_c = 7.52$ td(2); $\delta H_d = 7.11$ dd(2); $\delta H_{e,e'} = 2.19$ td(2), 3.75 ddd(2); $\delta H_{f,f'} = 3.39$ td(2), 3.26 ddd(2); $\delta H_{g,g'} = 3.16$ d(2), 2.14 d(2); $J_{a-b} = 6.00$; $J_{a-c} = 1.50$; $J_{b-c} = 7.80$; $J_{b-d} = 1.50$; $J_{c-d} = 7.80$; $J_{c-e} = 2.10$; $J_{e-e'} = 12.90$; $J_{e-f} = 12.90$; $J_{e-f'} = 12.90$; $J_{e'-f} = 5.10$; $J_{f-f'} = 2.10$; $J_{g-g'} = 9.90$, $\delta H_2 = 9.91$ s(2); $\delta H_5 = 8.24$ s(2); $\delta_{(3)}CH_3 = 2.80$ s(6); $\delta_{(4)}CH_3 = 2.81$ s(6)

^a δ , multiplicity, (integration), J /Hz.

complete oxidation of compound **1**; meanwhile when the scan potential was initiated in the negative direction, the chemical species formed after the electrolysis presents a very well-defined reversible electrochemical reduction process. A spectroelectrochemical study with an optical transparent thin layer electrode (OTTLE),³⁹ made of platinum minigrid, at potential 1.13 V/Fc–Fc⁺ was carried out. The experiment was monitored every 30 s (Figure 8 depicts results for 60 s intervals). A decrease of the absorbance in 358 nm MLCT ($d \rightarrow \pi^*$) and the appearance of a new band with maximum absorption at 525 nm during the electrolysis⁴⁰ suggest the oxidation of the central atom from Ru(II) to Ru(III). This transformation requires only one electron per molecule.

(39) DeAngelis, T. P.; Heineman, W. R. *J. Chem. Educ.* **1976**, *53*, 594–597.

(40) Ruiz-Ramirez, L.; Stephenson, T. A. *J. Chem. Soc., Dalton Trans.* **1973**, 1770–1782.

Table 7. ¹³C NMR Spectroscopic Data for Compounds 3–7


3	$\delta C_a = 153.9$; $\delta C_b = 123.8$; $\delta C_c = 138.3$; $\delta C_d = 127.4$; $\delta C_{a^*} = 150.6$; $\delta C_e = 26.6$; $\delta C_f = 31.6$; $\delta C_g = 34.0$; $\delta C_2 = \delta C_9 = 157.3$; $\delta C_3 = \delta C_8 = 127.0$; $\delta C_4 = \delta C_7 = 148.8$; $\delta C_5 = \delta C_6 = 125.8$; $\delta C_{11} = \delta C_{12} = 163.9$; $\delta C_{13} = \delta C_{14} = 135.5$; $\delta C(4)\phi = \delta_{o,m} 129.8$, $\delta_{p} 129.1$, $\delta_{\phi} 128.5$
4	$\delta C_a = 153.8$; $\delta C_b = 123.6$; $\delta C_c = 138.3$; $\delta C_d = 127.2$; $\delta C_{a^*} = 148.2$; $\delta C_e = 26.4$; $\delta C_f = 31.9$; $\delta C_g = 34.1$; $\delta C_2 = \delta C_9 = 157.6$; $\delta C_3 = \delta C_8 = 126.8$; $\delta C_4 = \delta C_7 = 138.7$; $\delta C_5 = \delta C_6 = 128.0$; $\delta C_{11} = \delta C_{12} = 163.8$; $\delta C_{13} = \delta C_{14} = 130.6$
5	$\delta C_a = 153.8$; $\delta C_b = 123.6$; $\delta C_c = 138.3$; $\delta C_d = 127.3$; $\delta C_{a^*} = 148.2$; $\delta C_e = 26.4$; $\delta C_f = 31.8$; $\delta C_g = 34.1$; $\delta C_2 = \delta C_9 = 156.4$; $\delta C_3 = \delta C_8 = 126.4$; $\delta C_4 = \delta C_7 = 135.4$; $\delta C_5 = 131.0 = \delta C_6$; $\delta C_{11} = \delta C_{12} = 163.8$; $\delta C_{13} = \delta C_{14} = 133.0$; $\delta C(5)CH_3 = 14.6$
6	$\delta C_a = 153.8$; $\delta C_b = 123.5$; $\delta C_c = 138.2$; $\delta C_d = 127.3$; $\delta C_{a^*} = 147.7$; $\delta C_e = 26.3$; $\delta C_f = 31.6$; $\delta C_g = 34.2$; $\delta C_2 = \delta C_9 = 157.0$; $\delta C_3 = \delta C_8 = 127.2$; $\delta C_4 = \delta C_7 = 149.2$; $\delta C_5 = \delta C_6 = 124.2$; $\delta C_{11} = \delta C_{12} = 163.8$; $\delta C_{13} = \delta C_{14} = 130.0$; $\delta C(4)CH_3 = 18.1$
7	$\delta C_a = 154.1$; $\delta C_b = 123.5$; $\delta C_c = 138.1$; $\delta C_d = 127.2$; $\delta C_{a^*} = 146.7$; $\delta C_e = 26.4$; $\delta C_f = 31.6$; $\delta C_g = 34.2$; $\delta C_2 = \delta C_9 = 157.7$; $\delta C_3 = \delta C_8 = 129.0$; $\delta C_4 = \delta C_7 = 146.9$; $\delta C_5 = \delta C_6 = 123.5$; $\delta C_{11} = \delta C_{12} = 163.8$; $\delta C_{13} = \delta C_{14} = 136.0$; $\delta C(3)CH_3 = 14.2$; $\delta C(4)CH_3 = 17.2$

Table 8. UV–Visible Spectroscopic Data for Compounds 3–7

compd	λ_{max} , nm (ϵ , M ⁻¹ cm ⁻¹)				
	MLCT ^{a,d}	LC ^{a,c,d}	MC ^a	MLCT ^b	MLCT ^a
3	238 (20841)	282 (27910)	no	320 (10927)	412 (5902)
4	235 (23425)	269 (25258)	295 (8789)	330 (7780)	400 (4835)
5	244 (5138)	276 (30136)	300 (13780)	328 (10530)	432 (5138)
6	239 (24135)	269 (24263)	294 (10364)	337 (8549)	397 (6301)
7	232 (21492)	273 (32071)	304 (11844)	334 (8489)	392 (7006)

^a Transition due to the coordination of 1,10-phenanthrolines. ^b Transition due to the coordination of pdto. ^c Intra-ligand LC ($\pi \rightarrow \pi^*$) transition.

^d In all complexes a transition at 252 nm LC ($\pi \rightarrow \pi^*$), due to pdto is also presented. ^{no} Not observed.

However, from the coulometric experiment two electrons per molecule were established, and there is one additional electron in the electrochemical process; thus the simultaneous oxidation of another chemical species during the electrolysis of **1** is presented. For this reason an electrochemical study of ligand in the absence of Ru(II) was performed. When the potential was started in the positive direction, only a single oxidation signal was observed at the anodic peak potential value of $E_{pa} = 0.63$ V/Fc–Fc⁺; when the scan was completed, no corresponding reduction signal peak was detected. By controlled potential coulometry at a potential value more positive than E_{pa} (0.83 V/Fc–Fc⁺), two electrons per molecule were established.

The simultaneous oxidation of Ru(II) and pdto must be discarded because three electrons per molecule would be

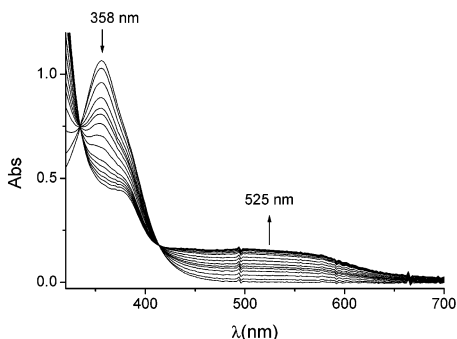


Figure 8. Spectroelectrochemical study in OTTLE made of platinum minigrad for 1 mM compound **1** (in the presence of 0.1 M TBABF₄ in acetonitrile) during controlled potential electrolysis at 1.13 V/Fc–Fc⁺. Each spectrum was acquired every 60 s.

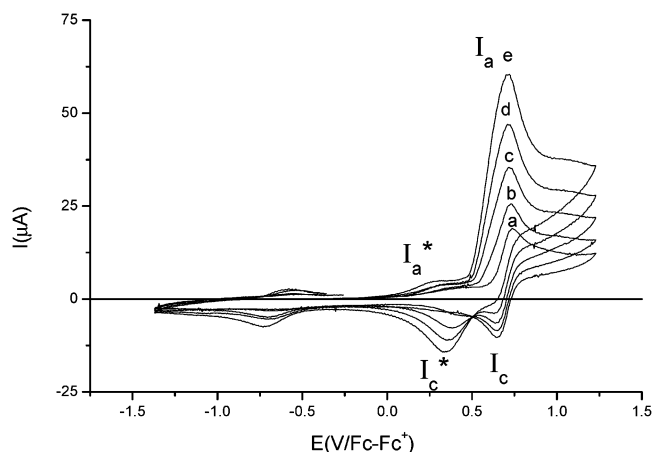


Figure 9. Cyclic voltammograms for 1 mM compound **1**, in the presence of 0.1 M TBABF₄ in acetonitrile. The scan potential was initiated from E_{ocp} to positive direction. Scan rate: 200 mV s⁻¹. Different amounts of ionic chloride as TBACl were added: (a) 0, (b) 1, (c) 2, (d) 3, and (e) 4 mM.

required, and the experimental evidence shows that only two electrons per molecule are involved in the oxidation of **1**. In order to explain these two electrons per molecule involved in this process, the simultaneous oxidation of Ru(II) and ionic chloride was proposed. To confirm this, cyclic voltammetric experiments of compound **1** in the presence of tetra-*N*-butylammonium chloride (TBACl), at different concentrations were carried out. When the ionic chloride was added, Figure 9, the currents associated with the oxidation (I_a) and reduction (I_c) signals clearly are increased, Figure 9b–d, while only a small increase of signals I_a^* and I_c^* was observed. Furthermore, a cyclic voltammetry experiment of a 1.40 mM new solution of compound **1** was obtained after warming to 353 K and then cooling to room temperature; an increase in the current associated with the oxidation (I_a) and reduction (I_c) signals was observed. This confirms the exchange of the coordinated chloride by acetonitrile releasing ionic chlorides for the oxidation process.

Electrochemistry of the Substituted Phenanthroline pdto Ru(II) Complexes. In all the electrochemical experiments, a 1 mM solution of each compound in supporting electrolyte (0.1 M TBATFB in acetonitrile) was used. Figure 10 shows a typical voltammogram of compound **4** obtained in a platinum electrode. When the potential scan was initiated in the negative direction, one reduction signal (I_c) was

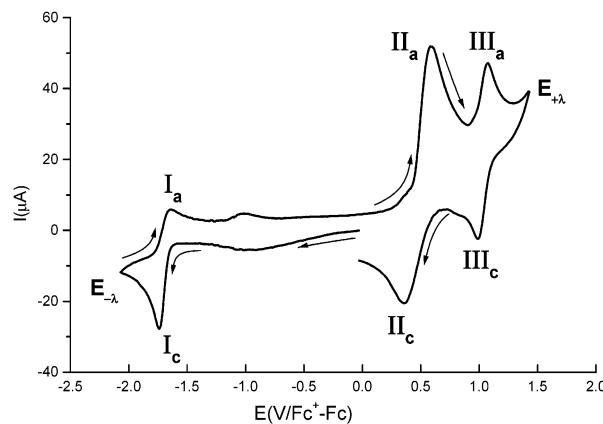


Figure 10. Cyclic voltammograms for 1.00 mM of compound **4** in the presence of 0.1 M TBABF₄ in acetonitrile. The scan potential was initiated from E_{ocp} to negative direction. Scan rate 1000 mV s⁻¹.

observed, and when the potential scan was reversed $E_{-λ}$, three oxidation signals (I_a , II_a , III_a) were observed. As the cycle was completed, two reduction signals (II_c , III_c) are also observed. On the other hand, when the potential scan was started in the positive direction, the same signals are observed; this fact demonstrates that signals II and III are independent of signal I. The independence of the oxidation signals II_a and III_a was established by modifying the switching potentials $E_{+λ}$. Each oxidation signal has respectively a corresponding reduction signal (II_c , III_c).

The cathodic peak potential value $E_{pc}(I)$ obtained for signal I_c was -1.733 V/Fc–Fc⁺, and the corresponding anodic peak potential value $E_{pa}(I)$ for signal I_a was -1.645 V/Fc–Fc⁺; a quasi-reversible electrochemical behavior is presented. The ΔE_p was independent of scan rate (0.1–1 V s⁻¹), and the cathodic peak current was proportional to $v^{1/2}$, indicating that process I is a diffusion-controlled process.⁴¹

The cathodic and anodic peak potential values for signals II_a and II_c $E_{pa}(II)$ and $E_{pc}(II)$ are 0.601 and 0.357 V/Fc–Fc⁺, respectively. The high ΔE_p indicates the presence of chemical reaction coupled to the electron transfer in process II.⁴¹

The anodic peak potential value $E_{pa}(III)$ obtained for signal III_a was 1.080 V/Fc–Fc⁺, and the cathodic peak potential value $E_{pc}(III)$ for signal III_c was 0.989 V/Fc–Fc⁺; a quasi-reversible electrochemical behavior is also observed.

In order to assign the electrochemical process associated with process I, a spectroelectrochemical study in optical transparent thin layer electrode (OTTLE)³⁸ was performed; the applied potential was -1.870 V/Fc–Fc⁺ (more negative than $E_{pc}(I)$), and the electrolysis was monitored every 30 s (Figure 11 depicts results for 60 s intervals). During the electrolysis, the absorbance decreased for all signals, particularly at 269 nm LC ($\pi \rightarrow \pi^*$); this is evidence of the reduction of the 1,10-phenanthroline ligand. A one-electron reduction for this process was established by controlled potential electrolysis. One-electron electrochemical reduction of 1,10-phenanthrolines coordinated to Ru(II) and Cu(II) have been reported.^{13,42}

(41) Bard, A. J.; Faulkner, L. R. *Electrochemical Methods, Fundamentals and Applications*; John Wiley and Sons: New York, 1980.

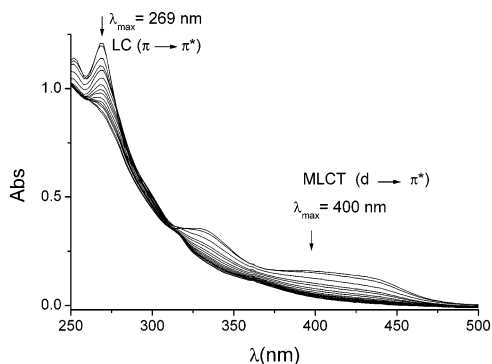


Figure 11. Spectroelectrochemical study in OTTLE made of platinum minigrad for 1 mmol dm⁻³ compound **4** (in the presence of 0.1 M TBABF₄ in acetonitrile) during controlled potential electrolysis at -1.87 V/Fc-Fc⁺. Each spectrum was acquired every 60 s.

A controlled potential coulometry at potential more positive than $E_{pa(II)}$ (0.700 V/Fc-Fc⁺) for a new solution of **4** established an oxidation of two electrons per molecule; no changes in the solution color were observed during the electrolysis. After electrolysis, disappearance of the electrochemical signal associated with process II was observed and the values of the peak potentials $E_{pa(I)}$, $E_{pc(I)}$ and $E_{pa(III)}$, $E_{pc(III)}$ remain unchanged. These facts suggest that process II corresponds to the oxidation of species outside the coordination sphere of the Ru(II); thus this process may correspond to the oxidation of the two ionic chloride atoms from complex **4**. This is in agreement with the fact that two electrons per molecule in the coulometric test at $E_{pa(II)}$ were obtained (one electron per chloride to form chlorine). In order to confirm this, cyclic voltammetric experiments of compound **4** in the presence of different amounts of tetra-*N*-butylammonium chloride (TBACl) were performed. When chlorides were added to the solution, an increase in the anodic and cathodic current peaks associated with electrochemical process II was observed; simultaneously the currents and the potentials associated with processes I and III remain unchanged. These facts confirm that this electrochemical process corresponds to the chloride ions. As it was previously demonstrated in complex **1** of this work, the electrochemical oxidation of the coordinated pdto ligand in the Ru(II) is not observed.

Finally, to obtain information of signal III, the solution recovered after controlled potential coulometry at $E_{pa(II)}$ was again electrolyzed at $E_{pa(III)}$, and one electron per initial molecule was established during the electrolysis. The solution color changes from yellow to green, and this fact suggests the oxidation of Ru(II) to Ru(III). This was confirmed by an spectroelectrochemical study, at 1.130 V/Fc-Fc⁺, Figure 12. The decrease of ligand metal charge transfer (MLCT) transitions bands (330 and 400 nm) for Ru(II) complex and the appearance of a new absorption maximum at 600 nm that corresponds to a Ru(III) compound were observed. The electrochemical behavior for compounds **3**, **5**, **6**, and **7** is very similar to that observed for **4**, though there are changes in the values of peak potentials; this will be discussed below.

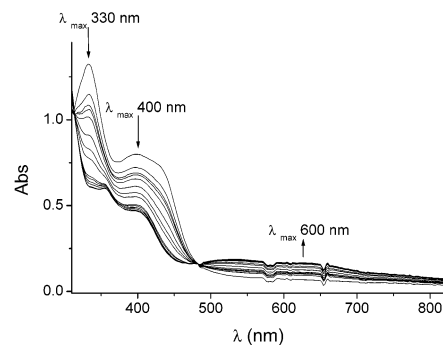


Figure 12. Spectroelectrochemical study in OTTLE made of platinum minigrad for 1 mM compound **4** (in the presence of 0.1 M TBABF₄ in acetonitrile) during controlled potential electrolysis at 1.13 V/Fc-Fc⁺. Each spectrum was acquired every 60 s.

Table 9. Electrochemical Potentials for Complexes **3–7**

compd	pK _a ^a	E _{1/2} ^b	
		Ru ^{II} /Ru ^{III}	phen/phen ⁻
3	4.8	1.042	-1.644
4	4.86	1.037	-1.689
5	5.6	1.050	-1.720
6	5.95	1.020	-1.805
7	6.31	0.997	-1.911

^a pK_a of free phenanthroline. ^b Redox potential, $E_{1/2} = (E_{pa} + E_{pc})/2$, reported vs ferrocene in 0.1 M TBABF₄-CH₃CN. Scan rate 1 V s⁻¹.

The half-wave potential was evaluated with the half sum of the anodic and cathodic peak potentials, $E_{1/2} = (E_{pa} + E_{pc})/2$, for the electrochemical processes III (Ru^{II}/Ru^{III}) and I (phen/phen⁻) for all the compounds.

Correlations. The $E_{1/2}$ (phen/phen⁻) and $E_{1/2}$ (Ru^{II}/Ru^{III}) values for each complex and the pK_a for each corresponding free substituted phenanthroline are listed in Table 9. In this table it is observed that the potential for the process (phen/phen⁻) increases linearly as the pK_a of the free substituted phenanthrolines increase; this demonstrates that the nature of the phenanthroline is determinant in the phen reduction process. This correlation between the potential $E_{1/2}$ (phen/phen⁻) in the complexes and the pK_a of free phenanthrolines was found to have the equation $E_{1/2} = -0.150 \text{ pK}_a - 0.9278$, with a correlation coefficient $r = 0.9432$. There have been reported correlations for Ru(II) polypyridine complexes in which the potential values $E_{1/2}$ (phen/phen⁻) are dependent on several properties of the free ligand, due to the nature, position, and number of substituents.¹³ Also Sanna and co-workers⁴² have obtained $E_{1/2}$ (phen/phen⁻) values for Cu(II) phenanthroline complexes, which have an inverse correlation with pK_a. The π*-acceptor properties of the phenanthrolines are not easily evaluated, but an experimental parameter widely accepted to indirectly measure these properties is the half-wave potential for the phen/phen⁻ reduction; moreover similar studies of quantitative analysis of ligands and effect (QALE) have suggested that the π*-acceptor properties of a ligand decrease regularly as their σ basicity increases.^{43,44} This is in agreement with our experimental evidence, i.e., the 4,7-diphenyl-1,10-phenanthroline ligand, in their corresponding complex (**3**), has a high π*-acceptor character (low

(42) Sanna, G.; Pio, M. I.; Zoroddu, M. A.; Seeber, R. *Inorg. Chim. Acta* **1993**, *208*, 153–158.

(43) Tollman, C. A. *Chem. Rev.* **1977**, *77*, 313–348.

(44) Drago, R. S.; Joerg S. *J. Am. Chem. Soc.* **1996**, *118*, 2654–2663.

pK_a) that causes a low potential $E_{1/2}$ (phen/phen⁻). On the other hand, the complex with 3,4,7,8-tetramethyl-1,10-phenanthroline (**7**) has a low π^* -acceptor character (high pK_a), which increases the potential $E_{1/2}$ (phen/phen⁻).

We also observed a linear correlation among the chemical shift of the ortho hydrogen δH_2 of the coordinated 1,10-phenanthroline, from Table 6, and the potential values $E_{1/2}$ of (phen/phen⁻). The equation obtained was $E_{1/2} = 0.588 \delta H_2 - 7.7543$ with a correlation coefficient $r = -0.989$. If the chemical shift measures the extent to which the nucleus is shielded, then this can be related to the acidity of the coordinated ligand. In this case shielding δH_2 of the ortho hydrogen nucleus can be also related to the π^* -acceptor character of the phenanthroline.

A rough tendency can also be observed for the potential (Ru^{II}/Ru^{III}) values with pK_a , Table 9. The complexes of the ligands with a higher pK_a show a low oxidation potential. This can be explained in terms of the stronger σ capability (higher pK_a) resulting in a higher electron density over the Ru(II) and consequently in a lower oxidation of the complexes. Within the context of ligand field theory, the correlation connecting the $E_{1/2}$ values of the complexes and the pK_a of the ligands has been attributed to the spherical density of the donor atoms at the antibonding d orbitals. Thus, complexes formed with ligands with high electron density on their donor atoms (high pK_a) will show lower $E_{1/2}$ values than those formed with weaker bases.⁴⁵ These correlations have been studied for Ru(II)–Schiff base complexes derived from substituted salicylaldehydes and triphenylphosphine.⁴⁶

A correlation can also be observed for the chemical shift of the ortho hydrogen δH_2 of the corresponding substituted 1,10-phenanthroline coordinated, and the $E_{1/2}$ (Ru^{II}/Ru^{III}) was obtained. This also suggests that the electrochemical potential (Ru^{II}/Ru^{III}) is a function of the electron density distribution produced by the substituent on the 1,10-phenanthrolines.

In order to obtain a correlation between the electrochemical and spectrochemical properties, the $E_{1/2}$ (Ru^{II}/Ru^{III}) and the λ_{max} of the MLCT absorption near 400 nm, were selected. The difference between $E_{1/2}$ of complex with nonsubstituted phenanthroline and $E_{1/2}$ of the complexes with substituted phenanthrolines is $\Delta E_{1/2}$; and the difference between λ_{max} of complex with nonsubstituted phenanthroline and λ_{max} of the

complexes with substituted phenanthrolines is $\Delta \lambda_{MLCT}$. A linear correlation was obtained with an equation $\Delta E_{1/2} = 0.0041 \Delta \lambda_{MLCT} + 0.0152$, and $r = 0.9554$.

Summary

A new compound **1** can be converted into **2** in acetonitrile solution by heating. This was confirmed by NMR studies, X-ray diffraction, and electrochemistry. The electrochemical behavior of compound **1** was studied by cyclic voltammetry, controlled potential coulometry, and spectroelectrochemical studies. The simultaneous oxidation of ionic chloride and Ru(II) was observed.

A new family of compounds with possible photochemical properties was synthesized and fully characterized by elemental analysis, X-ray diffraction, and NMR spectra. It was established by cyclic voltammetry, controlled potential coulometry, and spectroelectrochemical studies in acetonitrile that all these complexes present two oxidation processes: the oxidation of the ionic chlorides and the oxidation of the Ru(II). Additionally a mono-electronic reduction on the phenanthrolines coordinated to the Ru(II) was also observed. The electrochemical processes of the coordination compounds described in this work are affected by the electron-donating and electron-withdrawing properties of the ligands, due to the nature, number, and position of the substituents on the 1,10-phenanthroline. Stronger σ ability (higher pK_a) results in lower electron density over Ru(II) and consequently in a lower oxidation of the complexes. This was confirmed by the series of correlations between the $E_{1/2}$ Ru^{II}/Ru^{III} and the pK_a , δH_2 , and $\Delta \lambda_{max}$ (MLCT), respectively. The ligands Lⁿ with low pK_a will decrease the electron density in the rest of the molecule and consequently are easier to reduce and more difficult to oxidize.

Acknowledgment. The authors thank DGAPA-UNAM (IN212500) and CONACyT (3700PE) for financial support. L.A.O.-F. thanks CONACyT for a scholarship. M.A. thanks INTERCAMPUS and Intercambio Académico UNAM PROGRAM EXCHANGE for financial support from the exchange program. The authors thank USAI-Facultad Química UNAM and, particularly, G. Duarte, R. Del Villar, and O. Yañez for technical support.

Supporting Information Available: X-ray crystallographic file in CIF format for the structural determination of complexes **1a**, **2**, and **4**. This material is available free of charge via the Internet at <http://pubs.acs.org>.

IC025849Q

(45) Lintvedt, R. L.; Fenton D. E. *Inorg. Chem.* **1980**, *19*, 569–571.

(46) Marín-Becerra, A.; Ruiz-Ramírez, L.; Moreno-Esparza, R.; Del Río, P. J. F. *J. Coord. Chem.* **1993**, *29*, 359–370.